Nanotechnology **19** (2008) 375501 (11pp) doi:10.1088/0957-4484/19/37/375501

Carbon nanotube–TiO_2 hybrid films for detecting traces of O_2

E Llobet[1,6], E H Espinosa[1], E Sotter[1], R Ionescu[1], X Vilanova[1], J Torres[2], A Felten[3], J J Pireaux[3], X Ke[4], G Van Tendeloo[4], F Renaux[5], Y Paint[5], M Hecq[5] and C Bittencourt[5]

[1] MINOS, EMaS, Universitat Rovira i Virgili, 43007 Tarragona, Spain
[2] Research Department, Carburos Metálicos, MATGAS, Campus UAB, 08193 Cerdanyola del Vallès, Spain
[3] LISE, University of Namur, B-5000 Namur, Belgium
[4] EMAT, University of Antwerp, B-2020 Antwerp, Belgium
[5] LCIA, University of Mons-Hainaut, B-7000, Mons, Belgium

Received 3 June 2008, in final form 8 July 2008
Published 1 August 2008
Online at stacks.iop.org/Nano/19/375501

Abstract

Hybrid titania films have been prepared using an adapted sol–gel method for obtaining well-dispersed hydrogen plasma-treated multiwall carbon nanotubes in either pure titania or Nb-doped titania. The drop-coating method has been used to fabricate resistive oxygen sensors based on titania or on titania and carbon nanotube hybrids.

Morphology and composition studies have revealed that the dispersion of low amounts of carbon nanotubes within the titania matrix does not significantly alter its crystallization behaviour. The gas sensitivity studies performed on the different samples have shown that the hybrid layers based on titania and carbon nanotubes possess an unprecedented responsiveness towards oxygen (i.e. more than four times higher than that shown by optimized Nb-doped TiO_2 films). Furthermore, hybrid sensors containing carbon nanotubes respond at significantly lower operating temperatures than their non-hybrid counterparts. These new hybrid sensors show a strong potential for monitoring traces of oxygen (i.e. $\leqslant$10 ppm) in a flow of CO_2, which is of interest for the beverage industry.

1. Introduction

Due to their many advantages such as low cost, small size and robustness, semiconductor sensors appear to be good solution for oxygen trace detection. In some industrial processes such as the production of carbonated sodas and beers, the presence of oxygen must be detected and controlled in the ppm range. Some authors have reported the detection of oxygen at ppm levels using gas sensors [1, 2]. In most cases the sensors were developed employing thin film technology. However, in industrial applications, thick film technology is preferred due to its mature stage and lower costs when small/medium series of sensors are fabricated [1]. Furthermore, thick film technology is more flexible when small amounts of catalysts or sensitizers need to be added in the gas sensitive film [3–5]. Nevertheless, the detection of traces of oxygen remains a very difficult goal to reach using thick film sensors, and usually high operating temperatures (>700 °C) are needed. Although a titanium-dioxide-based thick film oxygen sensor working at 400 °C was reported by Sharma and co-workers [6], the detected oxygen concentration was near 1200 ppm, which is rather high for most applications (e.g. in the beverage industry).

Titanium dioxide has been the most widely used semiconductor material for oxygen detection [7–10]. Titania-based sensors (with the titania usually in the rutile phase) are bulk conductivity sensors. The oxygen detection mechanism implies the diffusion of oxygen ions in the bulk of the material, and this occurs provided the material is operated at high temperatures (700–1000 °C). This results in high power consumption, which is not desirable for most electronic applications.

In contrast, titania in the anatase crystalline phase has more free electrons than rutile titania [11]. For anatase titania, oxygen detection can be associated to a surface reaction, which takes place at lower temperatures (400–500 °C) [12, 13]. Keeping the anatase structure would allow for the detection of

[6] Author to whom any correspondence should be addressed.

oxygen at lower temperatures, which is desirable for sensor design [6, 14].

When titania is doped with pentavalent ions, e.g. Nb^{5+}, such ions get into the anatase titania crystalline structure, giving rise to a hindering in the phase transition to rutile and an inhibition in grain growth. While in undoped titania the change from anatase to rutile starts at about 600 °C, in doped titania, the transition temperature is higher, around 750 °C. This effect is attributed to the extra valence of niobium ions in comparison with titanium ones, which reduces the number of oxygen vacancies in the anatase phase, retarding the transformation to rutile [15–17].

Furthermore, grain growth is inhibited due to the stress induced in the anatase structure by the substitutional Nb^{5+} ions, which have a slightly higher ionic radius value with respect to Ti^{4+}. Smaller grains imply more active area, which increases the surface to volume ratio and thus the sensitivity [12, 17].

It has been reported that Nb-doped titania shows higher sensitivity towards oxygen and shorter response time than pure TiO_2 [18]. The doped material also shows lower impedance at low operating temperatures, and hence the design of the associated electronic circuitry is simpler [6]. In [15, 16] it was reported that an optimal value exists for the concentration of Nb in TiO_2. The best atomic ratio between Nb and Ti was found to be 3%. Recently, these materials were synthesized by a sol–gel route, calcined at different temperatures and had their oxygen sensing properties studied using nitrogen as balance gas [19]. It was found that a Nb-doped TiO_2 film calcined at 700 °C and operated at 500 °C was the most sensitive towards oxygen (10 ppm). The lower sensitivity shown by Nb-doped TiO_2 calcined at lower temperatures was attributed to a significant presence of the brookite crystalline phase in these samples. This phase is usually found before the formation of anatase (first) and then rutile crystalline states [20]. The brookite phase has fewer free carriers than anatase and its electrical behaviour is very like that of rutile [21]. Moreover, the lower sensitivity shown by Nb-doped TiO_2 calcined at temperatures higher than 700 °C was attributed to the fact that rutile becomes, by far, the dominant phase.

Multiwall carbon nanotubes (MWCNTs) have been recently employed as the active material in semiconductor gas sensors. The good potential of CNTs for detecting gases arises from their very large surface area because of their central hollow cores and outside walls. Recent studies have proved that MWCNT-based gas sensors can detect hazardous gases at low temperatures, and even at room temperature [22, 23]. This reduces the power consumption of the sensors and enables the safe detection of flammable gases in potentially explosive atmospheres. Therefore, this material is very promising as the active layer for gas sensing applications. Additionally, Collins and co-workers have shown that the electronic properties of single-wall carbon nanotubes are significantly affected by the presence of oxygen [24]. In the last few years, some authors have studied how the dispersion of functionalized carbon nanotubes within a metal oxide matrix results in hybrid films with gas sensing properties that compare favourably to those of the pure metal oxide. Wei and co-workers [25] reported on a hybrid film consisting of single-wall carbon nanotube bundles embedded in a tin oxide matrix. These hybrid films had higher response towards nitrogen dioxide and lower recovery times than pure tin oxide films when operated at room temperature. Zhao and co-workers [26] have reported on a hybrid film of multiwall carbon nanotubes coated with tin oxide nanoparticles with good sensitivity to carbon monoxide. Llobet and co-workers have shown that hybrid films consisting of oxygen plasma functionalized multiwall carbon nanotubes either dispersed in a tungsten oxide matrix [27] or coated with tungsten oxide nanoparticles [28] are highly responsive to nitrogen dioxide and ammonia at room temperature. Two main reasons are generally accepted for the enhanced sensitivity found in carbon nanotube and metal oxide hybrid films. These are the increase in the surface area of hybrid films and the stretching of the depletion layer at the metal oxide grain boundaries and at the CNT–metal oxide interface when the detected gases are absorbed [25–28].

In this work, films of pure titania, niobium-doped titania nanopowders and their corresponding hybrids with oxygen plasma functionalized multiwall carbon nanotubes were synthesized by a modified sol–gel route. In order to set the crystalline structure of the active materials, they were calcined at four different temperatures ranging from 500 to 800 °C. The materials obtained were characterized by different techniques. The objective of these characterizations was to obtain information about the material structure that could be related to its detection properties.

To determine the sensing properties of each material, they were deposited over alumina substrates that included contacts and a heater. Then they were tested under different concentrations of O_2 in CO_2 at different operating temperatures between 300 and 600 °C.

The organization of this paper is as follows. In section 2, the synthesis of the gas sensitive materials is discussed, details of the fabrication of the sensors are given and the methods employed to characterize the phase, morphology, composition and oxygen sensitivity of the active films are reviewed. In section 3 the results of the different characterizations are presented and discussed. Finally, a summary of the main results can be found in section 4.

2. Experimental details

2.1. Synthesis of gas sensitive materials

MWCNTs were employed to integrate some of the gas sensitive layers studied. Commercially available (Nanocyl, S.A. [29]) multiwalled carbon nanotubes grown by CVD were used. The as-provided nanotubes had purity higher than 95%, their length was up to 50 μm and their outer and inner diameters ranged from 3 to 15 nm and from 2 to 7 nm, respectively. In order to achieve better CNT dispersion in the TiO_2 matrix, the CNT powder was exposed to hydrogen plasma. The plasma treatment was carried out in an inductively coupled plasma operated at a frequency of 13.56 MHz [30]; the CNT powder was placed inside a glass vessel, and a magnet, externally controlled from the plasma chamber, was used to stir

the powder during the treatment. The treatment was performed at 0.15 Torr of hydrogen, with applied power equal to 30 W, and the treatment time was adjusted to 10 min.

Non-doped TiO_2 samples were synthesized through a sol–gel route, starting from an alkoxide precursor. Following the experiment done by Ruiz [17], titanium (IV) isopropoxide, also called tetraisopropyl orthotitanate $Ti[OCH(CH_3)_2]_4$, 99% purity, was mixed with isopropanol to get a 0.5 M solution to avoid early precipitations of oxides.

In the case of Nb-doped TiO_2, niobium ethoxide, $Nb(OC_2H_5)_5$ 99.99%, was also added to a 0.5 M solution of tetraisopropyl orthotitanate mixed with isopropanol in the appropriate concentration to obtain a Nb/Ti atomic ratio of 3%, which was the optimal doping concentration found by Arbiol [15, 16]. Because organic precursors were prone to oxidation, this process was conducted in N_2 atmosphere.

A solution of water and nitric acid, HNO_3 70%, was prepared in parallel. Then the mixture of organic precursors diluted in isopropanol was added dropwise to the acid solution under stirring. The final composition of the constituent was set to satisfy $[Ti]:[HNO_3]:[H_2O] = 1:1:100$ in molar ratio. In the case of hydrolysis–condensation of titanium isopropoxide, increasing the initial water concentration produced higher nucleation rates, which resulted in a decrease in average particle size. Nagpal and co-workers [31] showed that the main factor on particle size is the effect of water concentration. Based on this report, we selected a $[H_2O]/[Ti]$ ratio of 100. Because of the large amount of nitric acid, the hydrolysis proceeded without forming a precipitate, giving rise to a transparent sol at pH = 1.

Afterwards, the pH of the sol was increased carefully by adding dropwise approximately 30 ml of an aqueous solution (1 M) of ammonium hydrogen carbonate (pH = 9), until a consistent gel was achieved.

The gel was dried in an oven (UNE 300 from Memmert Co.). First, the temperature was set to 120 °C for 20 h to evaporate water. Then, temperature was increased to 250 °C for 10 h to eliminate some of the compounds generated during synthesis. Finally, the gel had a powdery appearance.

The sol–gel method described above was adapted to obtain titanium oxide and multiwall carbon nanotube hybrids. During the hydrolysis phase of the usual sol–gel preparation of TiO_2, a small quantity of plasma functionalized MWCNTs was introduced. The same procedure was also followed for obtaining Nb-doped TiO_2/MWCNT hybrids. After the nucleation process, the hybrid materials obtained presented a proportion of $\sim 1/500$ wt% MWCNT/TiO_2.

All the materials synthesized were subject to a firing process conducted at different temperatures. The firing was carried out in a programmable muffle (Carbilite RWF 1200). Each material synthesized was split in four parts to be fired in air at 500, 600, 700 and 800 °C, respectively. A temperature rise of 10 °C min^{-1} was applied to reach each firing temperature. Then, the samples remained at the firing temperature for 2 h. Finally, a free cooling rate was applied to the materials.

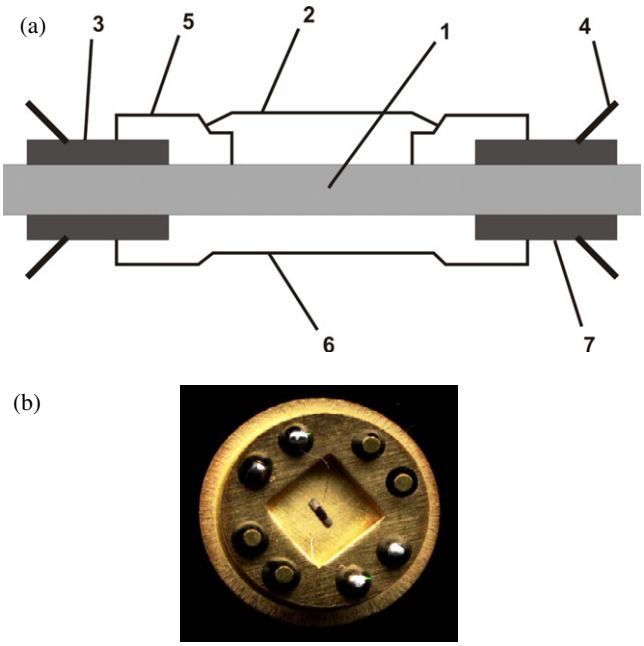

Figure 1. (a) Structure of the substrate. **1**, alumina substrate; **2**, sensing layer; **3**, Pt contact pads; **4**, connecting wires, **5**, ruthenium oxide diffusion barrier; **6**, Pt heater; **7**, Pt contact pads. (b) Picture of the actual device bonded to a standard TO-8 package.

(This figure is in colour only in the electronic version)

2.2. Sensor fabrication

The sensor substrate was fabricated by multilayer thick film deposition of a Pt-based heater, an insulation layer and contacts to the sensing layer. A ruthenium oxide diffusion barrier layer was employed to prevent interdiffusion between the Pt from the contact pads and the gas sensitive film. The use of a two-side construction (figure 1) allows for miniaturizing the sensor chip. The final dimensions of the sensor chip were 1.5 mm × 0.3 mm × 0.15 mm. The thickness of the alumina substrate was decreased down to 0.1 mm. The sensor chip was bonded to a TO-8 package. The diameter of the package was ∼10 mm [32].

The TiO_2-based nanopowders were dispersed in glycerol and then the resulting paste was dropped over the electrodes using a microinjector. The as-deposited films were dried at 300 °C using a temperature ramp. A temperature rise of 20 °C min^{-1} was used to avoid the occurrence of cracks in the metal oxide layer. Finally, the active layers were annealed for 2 h. Sensors whose active material had been calcined at 500 °C were annealed at 500 °C. The sensors that employed materials calcined at 600 °C or higher were annealed at 600 °C. The drying and annealing processes were made using the heating element of the sensors.

2.3. Film and sensor characterization

The total concentration of doping atoms (niobium atoms) in the doped titania was determined by using inductively coupled plasma optical emission spectroscopy (ICP-OES). ICP-OES was performed employing an OPTIMA 3200RL instrument

from Perkin Elmer. The radiofrequency source was set to 40 MHz and the operating power ranged between 750 and 1500 W. More details on how this analysis was performed can be found elsewhere [19].

The surface chemical composition of the films was investigated by x-ray photoelectron spectroscopy. XPS was performed using a VG-Escala 220 iXl instrument equipped with an Al Kα monochromatized x-ray beam by setting the electron energy analyser in the pass energy constant mode at a value of 20 eV. The voltage of the source was kept at 13 kV and spectra were collected at normal angle with respect to the sample surface. The spectroscope was calibrated at the Au 4f line at 84 eV. The energy resolution of the spectrometer for the Ag $3d_{5/2}$ line is about 0.5 eV.

The analysis of phase transition was studied by using x-ray diffraction (XRD). The measurements were made using a Siemens D5000 diffractometer (Bragg–Bretano parafocusing geometry and vertical θ–θ goniometer) fitted with a curved graphite diffracted-beam monochromator, incident and diffracted beam Soller slits, a 0.06° receiving slit and scintillation counter as a detector. The angular 2θ diffraction range was between 20° and 45°. The data were collected with an angular step of 0.05° at 3 s per step and sample rotation. Cu Kα radiation was obtained from a copper x-ray tube operated at 4 kV and 30 mA.

The morphology of the active layers was investigated using scanning electron microscopy (SEM). A Nova 200 Nanolab dual beam SEM/FIB and a Philips XL20 scanning electron microscope were used. Before SEM analysis, the samples were coated with a thin gold layer, which was sputtered to avoid charging effects. High resolution transmission electron microscopy (HRTEM) was performed using a Philips CM30-FEG microscope at 200 kV. For the TEM analyses the films were removed from the substrate using a razor blade and disposed on holey carbon-coated TEM support grids.

To study the oxygen sensing properties of the different sensors, these were placed in an airtight test chamber (with a volume of 16 cm^3). Three sensors of each material were employed for this experiment. Before starting a set of measurements, pure CO_2 (certified to contain less than 2 ppm of oxygen) was allowed to continuously flow through the measurement system for 12 h to ensure that the oxygen was flushed out. Every measurement consisted of two stages. In the first stage, pure CO_2 was let to flow through the test chamber and the sensor baseline was established. Then, a calibrated mixture of CO_2 and O_2 was mixed with pure CO_2 using mass-flow controllers and the resulting mixture was allowed to flow through the test chamber. The total flow was set constant to 140 ml min^{-1} during the whole measurement process. The accuracy of each mass-flow meter was +1% of its full scale. The sensors were tested at four different operating temperatures: 350 °C, 400 °C, 500 °C and 550 °C (only the first three temperatures were tested for those films that had been calcined at 500 °C). The change in resistivity of the active layers caused by the presence of oxygen was measured by employing a Keithley 6517A electrometer.

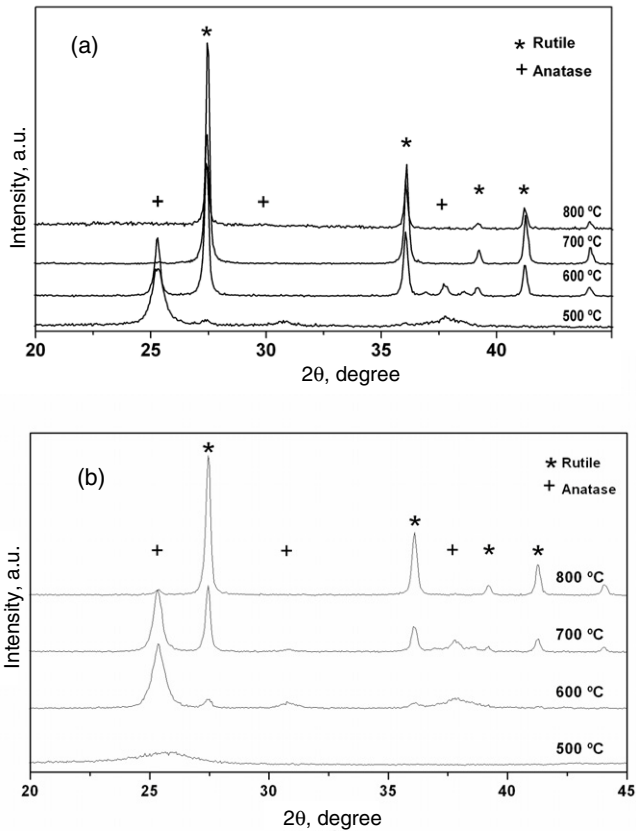

Figure 2. XRD patterns and quantitative analysis of films of titania–CNT (a) and Nb-doped titania–CNT (b), calcined at 500, 600, 700 and 800 °C.

3. Results and discussion

Film characterization

3.1. Structural and morphological analysis

XRD analysis performed on TiO_2–CNT films (see figure 2(a)) show that anatase is the dominant phase for materials annealed at 500 °C. While in TiO_2–CNT films annealed at 600 °C both the anatase and rutile phases coexist, in films annealed at 700 °C or higher rutile is the only phase present. From these results it can be stated that the phase transition in TiO_2–CNT films started at temperatures of about 500 °C. This early change of phase means an almost complete stabilization of its crystalline structure near 700 °C. This behaviour is in total concordance with that found in pure titania samples [19].

XRD analysis performed on niobium-doped TiO_2–CNT films show that anatase is the dominant phase for materials annealed up to 700 °C (see figure 2(b)). For the materials annealed at 500 and 600 °C a significant amount of the brookite phase is also present. It is only after being annealed at 800 °C that the rutile phase becomes dominant in niobium-doped TiO_2–CNT films. Once more, this behaviour is in total concordance with that found in niobium-doped titania samples [19]. During the doping process, Nb^{5+} ions enter substitutionally in the lattice, occupying Ti^{4+}

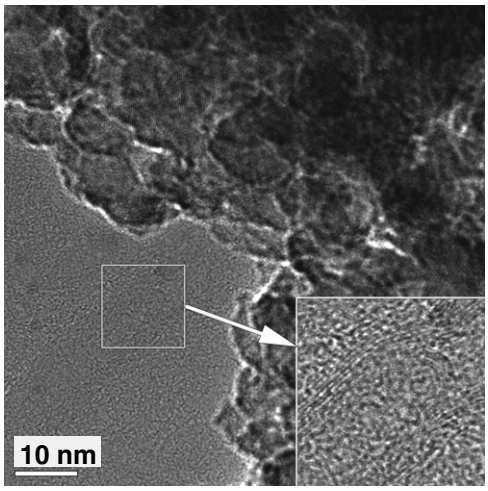

Figure 3. Nb-doped TiO_2–CNT annealed at 700 °C. Image showing the preserved CNT in the oxide matrix.

vacancies [33] without affecting the basic TiO_2 structure (anatase or rutile) [31] since the ionic radius of Nb^{5+} (0.70 Å) is comparable to that of Ti^{4+} (0.68 Å) [1, 6, 32, 33]. But, in order to assure the charge neutrality of the resulting material, these Nb^{5+} ions should be compensated by a decrease in the number of oxygen vacancies. In the anatase–rutile transformation, the anatase pseudo-close-packed planes of oxygen {112} are retained as the rutile close-packed planes {110}, and a cooperative rearrangement of titanium and oxygen ions occurs within this configuration [34, 37]. Oxygen vacancies placed in anatase planes act as nucleation sites for the anatase to rutile phase transformation [38], and therefore a minimum ratio of oxygen vacancies in anatase {112} planes is needed in order to assure the phase transition process. Then, the phase inhibition is attributed to the extra valence in niobium ions, which reduces oxygen vacancies in anatase phase, retarding the transformation to rutile [35–39].

XRD revealed that the inclusion of CNTs in the TiO_2 matrix had no effect on the phase transitions experienced by pure or niobium-doped titania as a function the annealing temperature. Therefore, TEM analyses were performed to verify whether CNTs resisted the film deposition process. Figure 3 shows high resolution TEM micrographs recorded on a Nb-doped TiO_2–CNT sample annealed at 700 °C. This image reveals the presence of nanotubes inside the TiO_2 film; apparently, the structure of the CNTs is not affected by the process employed to obtain the TiO_2–CNT hybrid films. To allow a better analysis of the CNTs embedded in the TiO_2 matrix, they were removed from the TiO_2 matrix by dissolving the film in ethanol in an ultrasonic bath. TEM images recorded on CNTs removed from the TiO_2 matrix are shown in figure 4; it can be seen that the CNT structure is preserved. The presence of nanoparticles attached to the CNT surface after nanotubes had been removed from the TiO_2 matrix reveals that they are strongly bonded to the CNT surface; EDX analysis confirmed the presence of carbon, titanium, oxygen and niobium.

3.2. Chemical composition of the films

3.2.1. ICP-OES analysis. The content of Nb in niobium-doped samples was estimated by ICP-OES analysis. This analysis revealed that the content of niobium in Nb-TiO_2 samples was 2.75 ± 0.2 at.%. In Nb-TiO_2–CNT hybrids, the content was estimated at 3.15 ± 0.2 at.%. These results are very close to the nominal value of 3 at.%.

3.2.2. XPS analysis. Since the chemical characteristics of the surface in anatase TiO_2 are decisive on the sensing properties, the chemical composition of the different gas sensitive films was investigated using XPS. Figure 5 shows typical XPS survey spectra recorded on TiO_2, TiO_2–CNT hybrid film and Nb-doped TiO_2–CNT hybrid film; for comparison a film prepared with just the hydrogen plasma-treated CNTs used to produce the TiO_2 matrix was also analysed. The two pronounced features in the spectrum recorded on the CNT film are generated by photoelectrons emitted from C 1s and O 1s core levels, respectively at 284.3 and 535 eV (figure 5(a)); the estimated oxygen concentration is 4%. The presence of oxygen at the CNT surface exposed to hydrogen plasma originates from residual gases in the treatment chamber.

Photoelectron peaks for Ti, O and C are present in all spectra recorded on the TiO_2-based films (figures 5(b) and (c)).

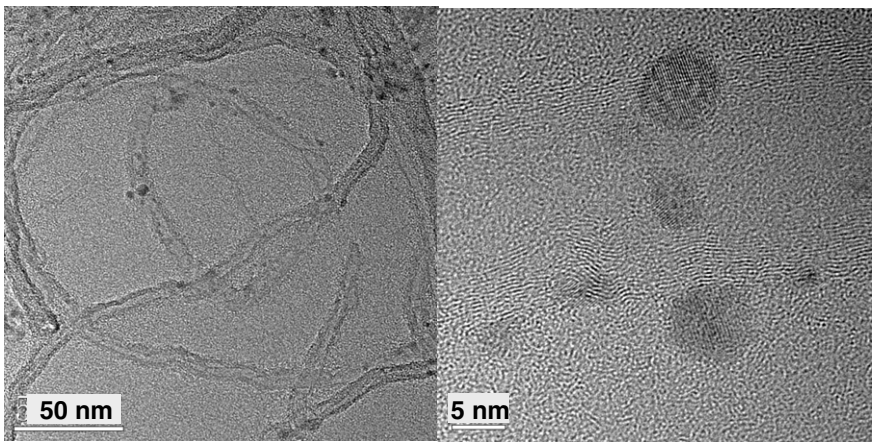

Figure 4. HRTEM image of CNT with TiO_2 nanoparticles attached.

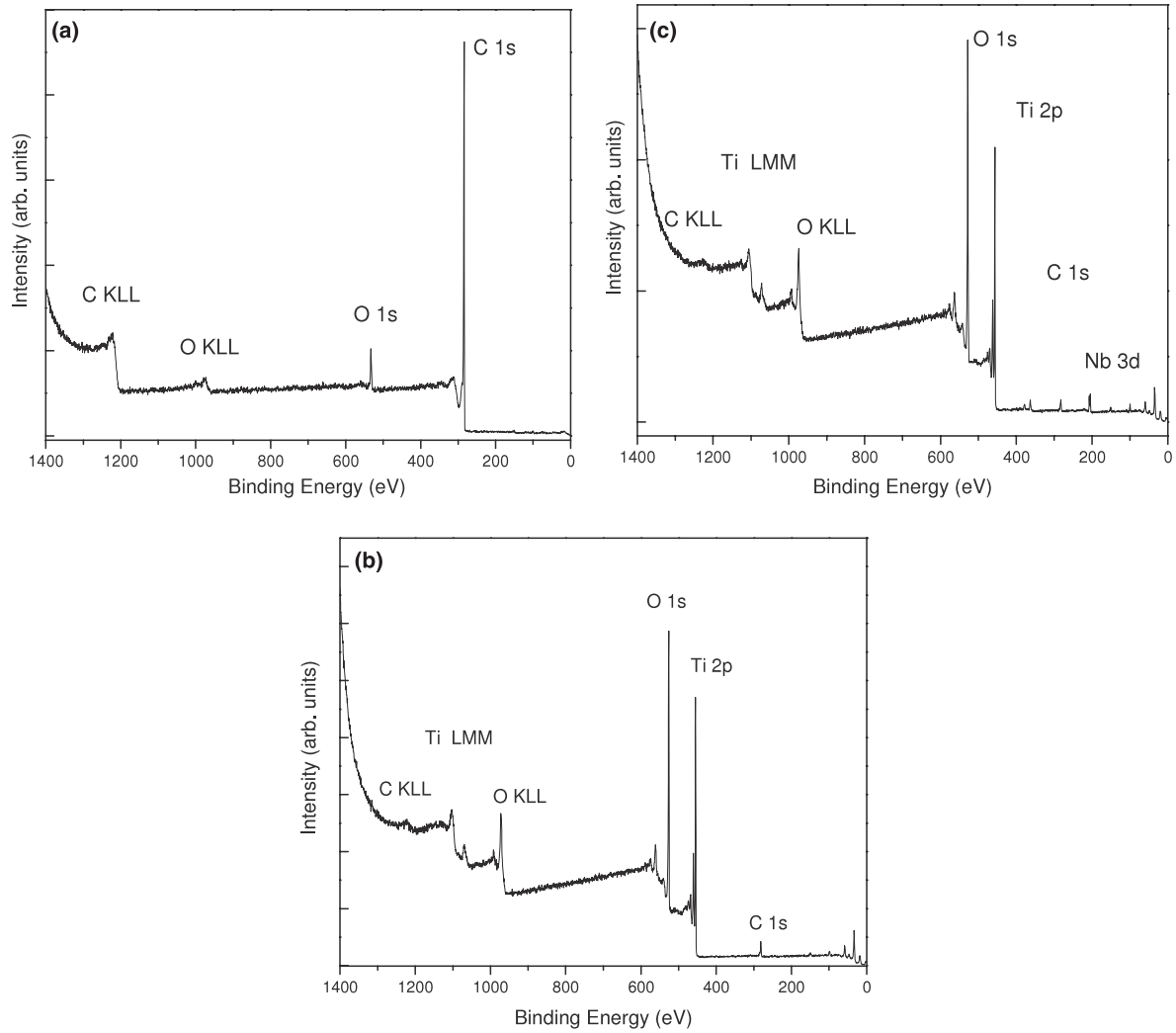

Figure 5. XPS survey spectra recorded on (a) CNT film, (b) CNT–TiO_2 film and (c) Nb-doped TiO_2–CNT.

In addition, on the XPS spectra recorded on films doped with Nb, peaks generated by photoelectrons emitted from the Nb 3d and Nb 3p core levels can be observed (figure 5(c)). Carbon and silicon are the main contaminants.

Identifying chemical modifications is straightforward when core levels are analysed. Figures 6(a), 7 and 8 show typical C 1s, Ti 2p, and O 1s core levels spectra recorded on the TiO_2-based samples. The C 1s peak main structure near 284.4 eV of binding energy corresponds to adventitious hydrocarbon species and incomplete decomposition of the carbon in the starting material [40]. The structure at higher binding energy is generated by photoelectrons emitted from carbon atoms belonging to hydroxyl groups (C–OH) and carboxyl groups (O=C–OH) [40]. For comparison, figure 6(b) presents the C 1s core level spectrum recorded on the hydrogen plasma functionalized CNT film; photoelectrons emitted from carbon atoms in the 'graphite-like' walls generate the main feature of these spectra at a binding energy of 284.3 eV. The absence of a pronounced structure at binding energy of 284.3 eV in the XPS spectra recorded on the CNT–TiO_2-based films indicates the absence of CNTs in the near surface region of the film. It is important to point out that the geometry used to record the XPS spectra (i.e., θ collect angle) was adjusted to obtain an analysis depth of 10 nm. Therefore, only photoelectrons originating from the surface up to this depth contribute to the signal. If a film of TiO_2 covers the CNTs the number of photoelectrons generated at the carbon nanotube surface that will contribute to the XPS signal will be reduced. Thus, the apparently low concentration of carbon in TiO_2–CNT hybrid films can be associated to the covering of the CNTs by the TiO_2 nanoparticles.

In agreement with the XPS results, in the SEM images recorded on the CNT–TiO_2 hybrid films there is no evidence of CNTs at the film surface. Figure 9 shows a typical SEM image: the surface of the films is made up of grains and voids. The grain size increases with increasing annealing temperature. In contrast, in agreement with the TEM results, CNTs can be observed inside the TiO_2 matrix if fractures of the surface are analysed. Figure 10 shows an image recorded through a fracture of the Nb-doped TiO_2–CNT film annealed at 700 °C: a section of a CNT standing outside the TiO_2 matrix can be observed. From the results discussed above, it can be said that CNTs are embedded in the TiO_2 matrix and there is no obvious agglomeration of CNTs inside or at the surface of the hybrid films.

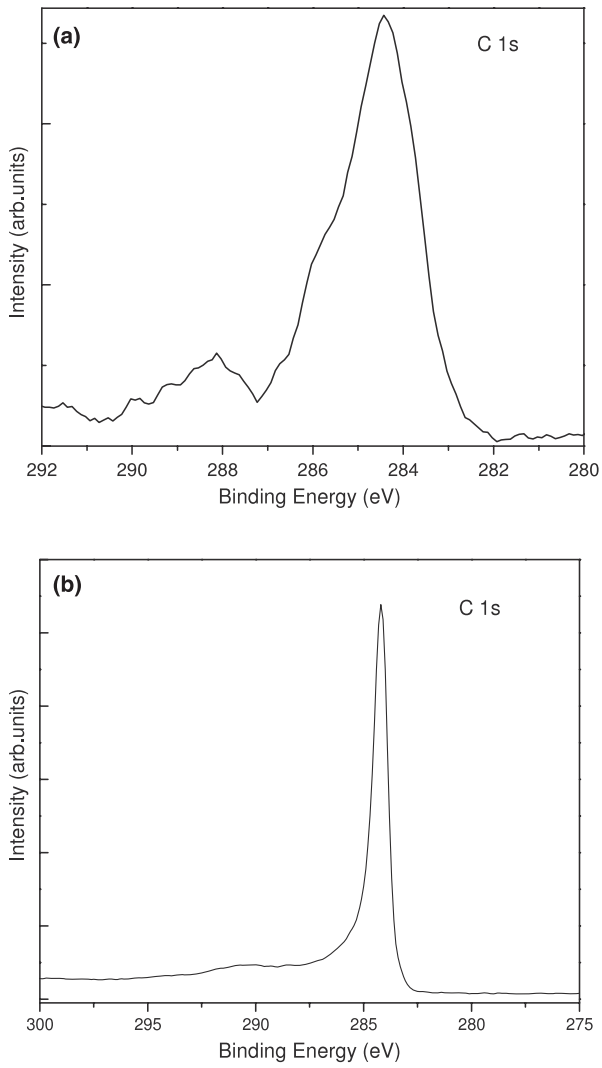

Figure 6. C 1s XPS spectra recorded on (a) CNT–TiO_2-based films and (b) CNT film.

In titanium oxide films, deviation from stoichiometry is likely to occur due to the various possible hybridization of the Ti 3d valence electrons with the O 2p ones. The oxidation state of TiO_2 films can be evaluated from the Ti 2p core level binding energy and spin–orbit splitting energy [41]. Figure 7, shows the typical Ti 2p doublet spectrum recorded on the TiO_2-based samples: the Ti $2p_{3/2}$ component at binding energy equal to 458.9 eV and the doublet separation energy equal to 5.6 eV indicate that the titanium ions have 4+ valence. The dominant feature in the O 1s XPS spectrum at 529.7 eV binding energy is generated by photoelectrons emitted from oxygen atoms in the TiO_2 matrix [42] (figure 8). The feature at higher binding energy can be mainly attributed to photoelectrons emitted from oxidized hydrocarbon. The atomic ratio of oxygen to titanium was measured to be 1.9 for the hybrid films and 2.0 for the TiO_2 films. No strong influence in the titanium oxidation state due to CNT addition to the TiO_2 matrix and/or Nb-doping was observed.

The Nb atomic concentration was measured to be near 1.5 for all samples. This value indicates that there is no Nb segregation to the sample surface.

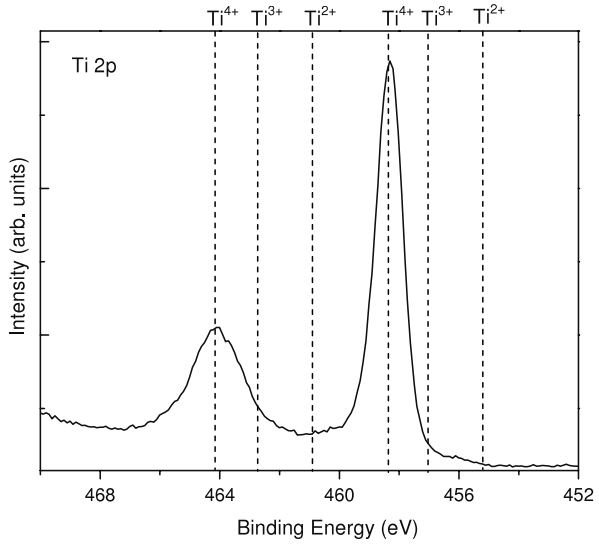

Figure 7. Ti 2p XPS core level spectrum recorded on the TiO_2-based films. The lines highlight the positions of the accepted binding energies for Ti in the 4+, 3+ and 2+ oxidation states [39].

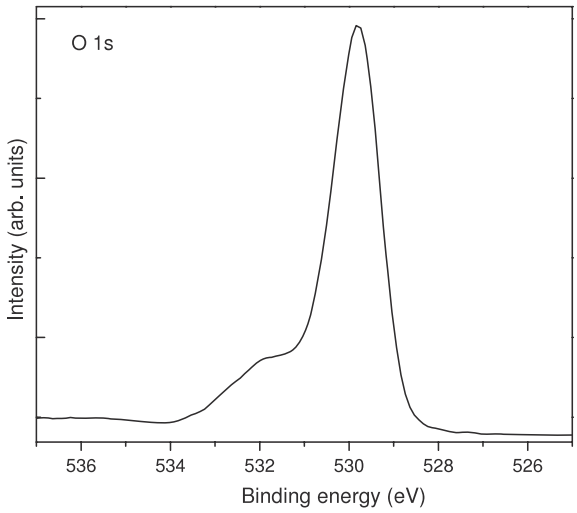

Figure 8. Typical O 1s XPS core level peak recorded on the TiO_2-based films.

3.3. Oxygen responsiveness studies

Responsiveness, R, was defined as follows: $R = \frac{R_{O_2} - R_{CO_2}}{R_{CO_2}}$, where R_{CO_2} is the baseline resistance of the sensor in a flow of CO_2 and R_{O_2} is the resistance of the sensor in the presence of 10 ppm of oxygen diluted in CO_2. The highest responsiveness towards oxygen among pure titania samples was for those calcined at 600 °C and operated at 500 °C. Their response towards 10 ppm of oxygen was equal to 0.2. Among the Nb-doped titania samples, only those calcined at 700 °C had good responsiveness towards oxygen, with responses between 1.1 and 1.6. The highest oxygen response was obtained when their operating temperature was set to 500 °C. In spite of the fact that the Nb-doped titania calcined at 600 °C had better physical characteristics (e.g. higher amount of anatase phase) than the one calcined at 700 °C, its responsiveness was poorer. A possible explanation for this low response may be the brookite

Table 1. Responsiveness and response time (min) to 10 ppm oxygen at different operating temperatures. The average values over three replicate measurements are shown and the errors (%) appear in brackets.

Material	Calcined at	Operated at	Responsiveness	Response time
TiO_2	600 °C	350 °C	0.12 (5.3)	3.0 (6.0)
		400 °C	0.13 (4.9)	2.5 (5.5)
		500 °C	0.20 (4.5)	2.0 (6.2)
		550 °C	0.14 (4.6)	1.5 (7.4)
Nb-TiO_2	700 °C [a]	350 °C	1.10 (5.5)	3.0 (7.0)
		400 °C	1.40 (5.3)	2.5 (6.5)
		500 °C	1.60 (4.3)	1.5 (5.4)
		550 °C	1.20 (4.5)	1.5 (6.8)
TiO_2 + CNT	600 °C	350 °C	6.50 (3.8)	8.0 (6.0)
		400 °C	4.20 (4.2)	7.0 (5.8)
		500 °C	1.90 (2.7)	5.0 (6.2)
		550 °C	1.50 (3.5)	5.0 (5.8)
Nb-TiO_2 + CNT	700 °C [a]	350 °C	2.50 (4.2)	7.0 (5.0)
		400 °C	2.20 (3.4)	6.0 (5.9)
		500 °C	1.10 (3.5)	5.0 (6.2)
		550 °C	0.60 (3.8)	5.0 (7.0)

[a] When calcined at 600 °C, the presence of a brookite phase results in a very low responsiveness (similar to that of pure titania).

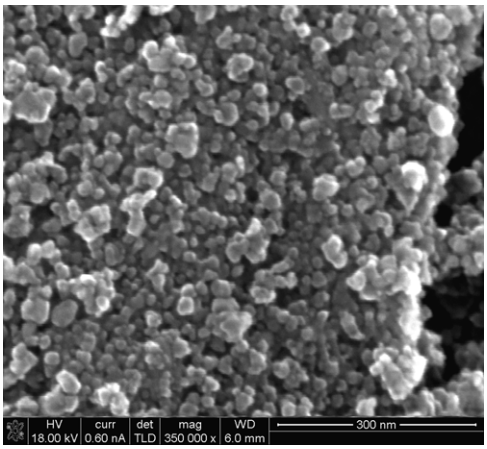

Figure 9. SEM image recorded on a Nb-doped TiO_2–CNT film.

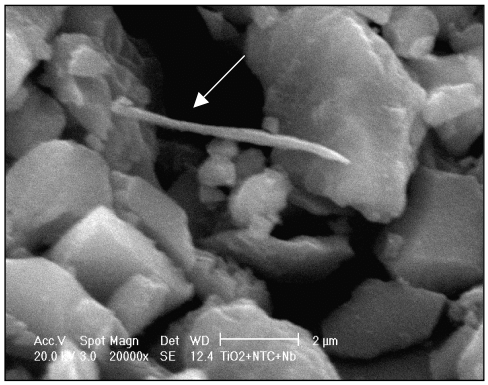

Figure 10. SEM image recorded on a fracture of the Nb-doped TiO_2–CNT film surface. The arrow indicates a TiO_2-covered CNT standing out of a fracture.

phase contained in the Nb-doped titania calcined at 600 °C; at this temperature the crystallinity of the brookite particles is improved with the consequent diminishing of surface defects, which affect the adsorption of oxygen species at the surface. That is, this result suggested that the occurrence of the brookite phase is even more detrimental than the presence of the rutile phase for the oxygen sensing properties of titania.

The presence of CNTs in the titania matrix had an important effect in the sensitivity towards oxygen. In TiO_2–CNT samples, the responsiveness (oxygen 10 ppm) ranged between 1.5 and 6.5. The highest responsiveness was obtained for samples calcined at 600 °C and operated at 350 °C. This response is more than four times higher than the one found for titania not containing carbon nanotubes and is reached at a significantly lower operating temperature. To our knowledge, this is the first time that such a high sensitivity has been reported at very low oxygen concentrations.

The responsiveness towards oxygen of hybrid sensors decreases with temperature for the temperature range studied. Too high an operating temperature can result in a lower adsorption of oxygen onto the hybrid film, which in turn results in a lower responsiveness [43].

In Nb-doped TiO_2–CNT samples, oxygen responsiveness ranged between 0.6 and 2.5, and the highest value was obtained for samples annealed at 700 °C and operated at 350 °C. Although this responsiveness outperforms that of Nb-doped titania, it remains lower than that of TiO_2–CNT samples. The fact that the presence of CNTs may alter the optimal value for the concentration of Nb in TiO_2 could explain this result. Figure 11 shows the responses to oxygen of different TiO_2–CNT-based sensors. The response in figure 11(a) is rather noisy and distorted because the value of sensor resistance is very high (>250 MΩ). While the 90% response time of sensors is below 5 min, the recovery of their baseline resistance takes about 20 min when the sensors are operated at 350 °C. Recovery times can be speeded up by operating the sensors at higher operating temperature during the cleaning phase. Table 1 summarizes the oxygen responsiveness results. Only the best

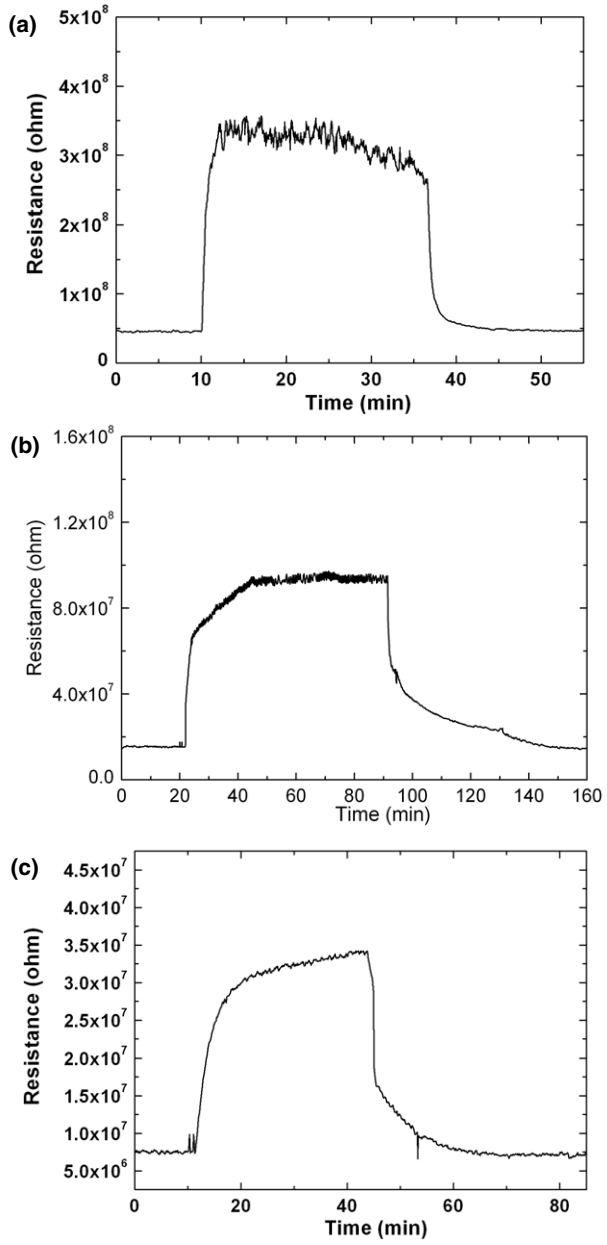

Figure 11. Response to 10 ppm of O_2 in CO_2 flow for a TiO_2/MWCNT sensor sintered at 500 °C (a), a TiO_2/MWCNT sensor sintered at 600 °C (b) and a Nb-doped TiO_2/MWCNT sensor sintered at 500 °C (c). All sensors were operated at 450 °C.

results for each one of the four different materials considered are reported in this table (i.e., results for the optimal annealing temperature of each material).

3.4. Oxygen sensing mechanism

On the basis of the electron microscopy images (shown in figure 3, 4 and 10) recorded on the different hybrid films investigated, it can be derived that the morphology of the hybrid films is characterized by an overlayer formed by TiO_2 particles anchored at the surface of a mesh of well-dispersed MWCNTs. Figure 4 reveals that the external wall of CNTs is covered with TiO_2 particles. Therefore, the hybrid films can be considered as MWCNTs embedded in a TiO_2 matrix. Since TiO_2 behaves as an n-type semiconductor and MWCNTs can be considered to behave as p-type semiconductors [25, 40] the heterostructure n-TiO_2/p-MWCNTs can be formed at the interface between titania and carbon nanotubes. In such hybrid films, two different depletion layers (and associated potential barriers) can coexist [25, 28]. The first type of depletion layer is located at the surface of the grains of the metal oxide film and the second type at the interface between MWCNTs and metal oxide films. While the first depletion layer is caused by the adsorption of ionized oxygen at the surface of titania grains, the second one is caused by the metal oxide/carbon nanotube heterojunction.

Considering the gas sensing results presented in this paper, it can be derived that the adsorption of oxygen at the surface of titania grains modifies the width of the first depletion layer (i.e., the one at the surface of metal oxide grains), which in turn alters the depletion layer at the n-TiO_2/p-MWCNT heterostructure.

Hybrid sensors are significantly more responsive to oxygen than pure or Nb-doped titania sensors because a slight change in the concentration of adsorbed oxygen at its surface (i.e., a slight change in the first depletion layer) can result in a significant change in the depletion layer at the n-TiO_2/p-MWCNT heterostructure. This implies a significant change in the resistance of the hybrid sensor (i.e. an amplification effect occurs in the change of resistance). In [24] Collins and co-workers demonstrated that the electrical conductance of single-wall carbon nanotubes heavily depends on the physical and/or chemical adsorption of oxygen on CNTs. In our samples the TiO_2 matrix is porous, and oxygen could diffuse through its pores and reach the surface of the nanotubes. Therefore, the increase in sensitivity of hybrid sensors could be due in part to the adsorption of oxygen on MWCNTs.

4. Conclusions

An adapted sol–gel method has been introduced for obtaining well-dispersed hydrogen plasma-treated multiwall carbon nanotubes in a matrix of either pure titania or Nb-doped titania. The drop-coating method has been used to fabricate resistive oxygen sensors based on titania or on titania and carbon nanotube hybrids.

Structural and composition studies such as XRD, XPS and ICP have revealed that the dispersion of low amounts of carbon nanotubes within titania does not significantly alter the crystallization behaviour of the latter (e.g. phase transitions occur in similar intensities and at equal temperatures in titania and in carbon nanotube-containing titania). While the surface of the films consists of an overlayer of TiO_2, electron microscopy analyses have shown that carbon nanotubes are present embedded in the titania matrix. Furthermore, HRTEM studies reveal that the carbon nanotube structure is not affected by the sol–gel and the drop-coating methods employed to obtain sensors (e.g. these methods employ thermal treatments either in inert or in reactive ambient).

The gas sensitivity studies performed on the different samples have shown that the hybrid layers based on titania and

carbon nanotubes possess an unprecedented responsiveness towards oxygen (i.e. more than four times higher than that shown by optimized Nb-TiO_2 films). Furthermore, hybrid sensors containing carbon nanotubes respond at significantly lower operating temperatures than their non-hybrid counterparts. The fact that the presence of CNTs may alter the optimal value for the concentration of Nb in TiO_2 could explain why TiO_2–CNT-based sensors outperformed those based on Nb-doped TiO_2–CNT films in this study.

Based on these results, the modulation of the width of two depletion layers existing at the surface of titania grains and at the interface of titania grains and MWCNTs, respectively, is postulated as the mechanism that could explain the enhanced performance of hybrid TiO_2/MWCNT sensors in comparison with pure metal oxide sensors. The direct adsorption of oxygen on MWCNTs could also explain in part the increase in sensitivity shown by hybrid sensors.

These new hybrid sensors show good potential for monitoring traces of oxygen (i.e. $\leqslant$10 ppm) in a flow of CO_2, which is of interest for the beverage industry.

Acknowledgments

This work has been funded by Carburos Metálicos S.A., the Belgian Programme on Interuniversity Attraction Pole (PAI 6/08), the 'Actions de recherche concertées (ARC)' and by EC-FP6-STREP-033311 Nano2hybrids project.

References

[1] Sharma R K and Bhatnagar M C 1999 Improvement of the oxygen gas sensitivity in doped TiO_2 thick films *Sensors Actuators* B **56** 215–9
[2] Hu Y, Tang O K, Pan J S, Huang H and Cao W 2005 The effect of annealing temperature on the sensing properties of low temperature nano-sized $SrTiO_3$ oxygen gas sensor *Sensors Actuators* B **108** 244–9
[3] Guidi V, Butturi M A, Carotta M C, Cavicchi B, Ferroni M, Malagù C, Martinelli G, Vincenzi D, Sacerdoti M and Zen M 2002 Gas sensing through thick film technology *Sensors Actuators* B **84** 72–7
[4] Ivanov P, Llobet E, Vilanova X, Brezmes J, Hubalek J and Correig X 2004 Development of high sensitivity ethanol gas sensors based on Pt-doped SnO_2 surfaces *Sensors Actuators* B **99** 201–6
[5] Ivanov P, Llobet E, Blanco F, Vergara A, Vilanova X, Gracia I, Cane C and Correig X 2006 On the effects of the materials and the noble metal additives to NO_2 detection *Sensors Actuators* B **118** 311–7
[6] Sharma R K, Bhatnagar M C and Sharma G L 1998 Mechanism in Nb doped TiO_2 oxygen gas sensor *Sensors Actuators* B **46** 194–201
[7] Kirner U, Schierbaum K D, Gopel W, Leibold B, Nicoloso N, Weppner W, Fischer D and Chu W F 1990 Low and high-temperature TiO_2 oxygen sensors *Sensors Actuators* B **1** 103–7
[8] Sheng J, Yoshida N, Karasawa J and Fukami T 1997 Platinum-doped titania films oxygen sensor integrated with temperature compensating thermistor *Sensors Actuators* B **41** 131–6
[9] Takami A 1988 Development of titania heated exhaust gas oxygen sensor *Ceram. Bull.* **67** 1956–60
[10] Azad A M, Akbar S A, Mhaisalkar S G, Birkefeld L D and Goto K S 1992 Solid-state gas sensors: a review *J. Electrochem. Soc.* **139** 3690–5
[11] Tang H, Prasad K, Sanjinés R and Lévy F 1995 TiO_2 anatase thin films as gas sensors *Sensors Actuators* B **26** 71–5
[12] Xu Y, Zhou X and Sorensen O T 2000 Oxygen sensors based on semiconducting metal oxides: an overview *Sensors Actuators* B **65** 2–4
[13] Zakrzewska K 2004 Gas sensing mechanism of TiO_2-based thin films *Vacuum* **74** 335–8
[14] Hossein-Babaei F, Keshmiri M, Kakavand M and Troczynski T 2005 A resistive gas sensor based on undoped p-type anatase *Sensors Actuators* B **110** 28–35
[15] Arbiol J 2001 Metal additive distribution in TiO_2 and SnO_2 semiconductor gas sensor nanostructured materials *Doctoral Thesis* Universitat de Barcelona, Departament d'Electrònica
[16] Arbiol J, Cerdà J, Dezanneau G, Cirera A, Peiró F, Cornet A and Morante J R 2002 Effects of Nb doping on the TiO_2 anatase-to-rutile phase transition *J. Appl. Phys.* **92** 853–61
[17] Ruiz A, Dezanneau G, Arbiol J, Cornet A and Morante J R 2003 Study of the influence of Nb content and sintering temperature on TiO_2 sensing films *Thin Solid Films* **436** 90–4
[18] Sharma R K 1996 Development and characterization solid state materials for oxygen gas sensors *Doctoral Thesis* Indian Institute of Technology, Department of Physics
[19] Sotter E, Vilanova X, Llobet E, Vasiliev A and Correig X 2007 Thick film titania sensors for detecting traces of oxygen *Sensors Actuators* B **127** 567–79
[20] Djaoued Y, Brüning R, Bersani D, Lottici P P and Badilescu S 2004 Sol–gel nanocrystalline brookite-rich titania films *Mater. Lett.* **58** 2618–22
[21] Koelsch M, Cassaignon S, Ta C, Minh T, Guillemoles J F and Jolivet J P 2004 Electrochemical comparative study of titania (anatase, brookite and rutile) nanoparticles synthesized in aqueous medium *Thin Solid Films* **451/452** 86–92
[22] Varghese O K, Kichambre P D, Gong D, Ong K G, Dickey E C and Grimes C A 2001 Gas sensing characteristics of multi-wall carbon nanotubes *Sensors Actuators* B **81** 32–41
[23] Wang S G, Zhang Q, Yang D J, Sellin P J and Zhong G F 2004 Multiwalled carbon nanotube-based gas sensors for NH_3 detection *Diamond Relat. Mater.* **13** 1327–32
[24] Collins P G, Bradley K, Ishigami M and Zettl A 2000 Extreme oxygen sensitivity of electronic properties of carbon nanotubes *Science* **387** 1801–4
[25] Wei B-Y, Hsub M-C, Su P-G, Lin H-M, Wu R-J and Lai H-J 2004 A novel SnO_2 gas sensor doped with carbon nanotubes operating at room temperature *Sensors Actuators* B **101** 81–9
[26] Zhao L, Choi M, Kim H-S and Hong S-H 2007 The effect of multiwalled carbon nanotube doping on the CO gas sensitivity of SnO_2-based nanomaterials *Nanotechnology* **18** 445501
[27] Bittencourt C, Felten A, Espinosa E H, Ionescu R, Llobet E, Corteig X and Pireaux J J 2006 WO_3 films modified with functionalised multi-wall carbon nanotubes: morphological, compositional and gas response studies *Sensors Actuators* B **115** 33–41
[28] Espinosa E H *et al* 2007 Highly selective NO_2 gas sensors made of MWCNTs and WO_3 hybrid layers *J. Electrochem. Soc.* **154** J141–9
[29] http://www.nanocyl.com
[30] Lefebre C and Verbist J 1992 *Adv. Comput. Mater. Lett.* **1** 34
[31] Nagpal V J, Davis R M and Riffle J S 1994 *In situ* steric stabilization of titanium dioxide particles synthesized by a sol–gel process *Colloids Surf.* A **87** 25–31

[32] Kim J H, Sung J S, Son Y M, Vasiliev A A, Malyshev V V, Koltypin E A, Eryshkin A V, Godovski D Y, Pisyakov A V and Yakimov S S 1997 Propane/butane semiconductor gas sensor with low power consumption *Sensors Actuators* B **44** 452–7

[33] Zimmermann P H 1973 Temperature dependence of the EPR spectra of niobium-doped TiO_2 *Phys. Rev.* B **8** 3917–27

[34] Bernasik A, Radeeka M, Rekes M and Sloma M 1993 Electrical properties of Cr and Nb doped TiO_2 thin films *Appl. Surf. Sci.* **65/66** 240–5

[35] Carotta M C, Ferroni M, Gnani D, Guidi V, Merli M, Martinelli G, Casale M C and Norato N 1999 Nanostructured pure and Nb-doped TiO_2 as thick film gas sensors for environmental monitoring *Sensors Actuators* B **58** 310–7

[36] Ferroni M, Carotta M C, Guidi V, Martinelli G, Ronconi F, Richard O, Dyck D V and Landuyt J V 2000 Structural characterization of Nb-TiO_2 nanosized thick-films for gas sensing application *Sensors Actuators* B **68** 140–5

[37] Shannon R D and Pask J A 1965 Kinetics of the anatase–rutile transformation *J. Am. Ceram. Soc.* **48** 391–8

[38] Hishita S, Mutoh I, Koumoto K and Yanagida H 1983 Inhibition mechanism of the anatase–rutile phase transformation by rare earth oxides *Ceram. Int.* **9** 61–7

[39] Akhtar M K, Pratsinis S E and Mastrangelo S V R 1992 Dopants in vapor-phase synthesis of titania powders *J. Am. Ceram. Soc.* **75** 3408–16

[40] Moulder J F, Stickle W F, Sool P E and Bomben K D 1992 *Handbook of X-ray Photoelectron Spectroscopy* (Eden Prairie, MN: Perkin-Elmer)

[41] Turkovic A and Sokcevic D 1993 X-ray photoelectron spectroscopy of thermally treated TiO_2 thin films *Appl. Surf. Sci.* **68** 477–9

[42] Wagner C D, Gale L H and Raymond R H 1979 Two-dimensional chemical state plots: a standardized data set for use in identifying chemical states by x-ray photoelectron spectroscopy *Anal. Chem.* **51** 466–82

[43] Valentini L, Armentano I, Kenny J M, Cantalini C, Lozzi L and Santucci S 2003 Sensors for sub-ppm NO_2 gas detection based on carbon nanotube thin films *Appl. Phys. Lett.* **82** 961–3